35th Annual International Conference of the IEEE EMBS
Osaka, Japan, 3 - 7 July, 2013

Polycarbazole-based Organic Photodiodes for Highly Sensitive Chemiluminescent Immunoassays*

Nuno M. M. Pires, and Tao Dong, *Member, IEEE*

Abstract— **It is reported the development of a polycarbazole-based organic photodetector for chemiluminescent immunoassays. The optical detector comprised a 1:4 blend by weight of poly [N-9`-heptadecanyl-2,7-carbazole-alt-5,5-(4`,7`-di-2-thienyl-2`,1`,3`-benzothiadiazole)] (PCDTBT) and [6,6]-phenyl C_{71}-butyric acid methyl ester ($PC_{70}BM$). Optimization of the photodetector design was conducted aiming to maximize photosensitivity and reduce the background level. Quantitation of recombinant human thyroid stimulating hormone indicated good linearity and yielded a detection sensitivity of ~3.7 $nA \times nM^{-1}$ and a detection limit of 80 pg/ml.**

I. Introduction

Practical utilization of point-of-care (POC) diagnostics has faced challenges in integrating low-cost, sensitive, and miniaturized optical detection systems. Although several works have reported microfluidic devices incorporating optical detection using conventional CCD or CMOS image sensors [1, 2], these systems do not translate well to robust POC devices. Potential detectors for POC optical sensors include silicon photodetectors and organic photodetectors (OPDs). Silicon optical detectors are considered sensitive for detection of low analyte concentrations. However, the use of silicon photodiodes and micromachined silicon substrates involves high-cost fabrication techniques that hinder the use of such devices as disposable sensors. The emergence of organic/polymer electronic devices that can be realized by simple low-cost fabrication methods, including spin-coating, inkjet printing, and spray-coating, may offer new prospects in POC technology. Organic photodiodes can be printed onto flexible substrates, which is a key advantage of these photodetectors over their silicon-based counterparts. In addition, an OPD requires simple readout instrumentation, as the photodiode can be fully integrated with microfluidic chip structures.

The performance of organic photodiodes for light-sensing applications depends on their dark current and photon collection or quantum efficiency. Minimizing the dark current and maximizing the quantum efficiency for a desired wavelength range are important steps to enhance the detection limit (LOD) and detection sensitivity of biosensors. Fluorescence and chemiluminescence based sensors incorporating OPDs have been reported in recent works. Pais et al. [3] have developed an integrated microfluidic system for fluorescence detection with an organic light-emitting diode and an organic photodiode made of $CuPC/C_{60}$. Wang et al. [4] have developed a chemiluminescence detection system for hydrogen peroxide and antioxidants using a photodiode fabricated with a blend heterojunction of poly(3-hexylthiophene) (P3HT) and [6,6]-phenyl C_{61}-butyric acid methyl ester ($PC_{60}BM$).

Recently, new classes of semiconducting polymers have been developed to achieve much better stability under ambient conditions and enhanced optoelectronic characteristics. Among them, poly(2,7-carbazole) derivatives, especially poly [N-9`-heptadecanyl-2,7-carbazole-alt-5,5-(4`,7`-di-2-thienyl-2`,1`,3`-benzothiadiazole)] (PCDTBT), have demonstrated their potential as a series of promising alternative materials to P3HT in organic solar cell applications. The combination of PCDTBT with fullerene derivatives as blend heterojunction devices yields superior power conversion efficiencies [5]. PCDTBT photovoltaic devices have exhibited a higher short circuit current (J_{sc}) comparing to P3HT based detectors, which makes them interesting for low-intensity light sensing applications.

Here, a blend heterojunction PCDTBT:$PC_{70}BM$ device was developed as a novel photodetector for chemiluminescent biosensors. Chemiluminescence based detection is preferred for POC diagnostic applications as it precludes an external light source, thereby lowering instrument costs and significantly reducing background interference compared to fluorescence assays. As proof-of-concept experiments, an immunoassay sensing scheme was set to detect recombinant human thyroid stimulating hormone (rhTSH), which has an important diagnostic use in patients with thyroid cancer.

II. Materials & Methods

The schematic of the chemiluminescent biosensor is shown in Fig. 1. It comprises the organic photodiode and the chemiluminescent reaction chip, excluding the use of optical lenses or filters that are difficult to miniature into a low-cost, portable and robust biosensor [1]. The reaction chip was realized by sputtering the bilayer Au (200 nm thick)/Ti (20 nm thick) [6, 7] as the reflective coating on top of the Pyrex 7740 glass wafer.

*Research mainly supported by Norsk regional kvalifiseringsstøtte fra Oslofjorfondet (Et cellebasert digitalt mikrofluidisk system, proj. 220635) and Research Council of Norway via the support to the Norwegian Micro- and Nano-Fabrication Facility, NorFab (197411/V30), Norwegian long term support from NorFab project.

T. Dong (IEEE member nr. 90889664) is with the Department of Micro and Nano Systems Technology - IMST, TekMar, Vestfold University College - HiVe, Postboks 2243 N-3103 Tønsberg, Norway (corresponding author to provide phone: +47-3303-7731; fax: +47-3303-1103; e-mail: Tao.Dong@hive.no).

Nuno M. M. Pires is with the Department of Micro and Nano Systems Technology - IMST, TekMar, Vestfold University College - HiVe, Postboks 2243 N-3103 Tønsberg, Norway (e-mail: Nuno.Pires@hive.no).

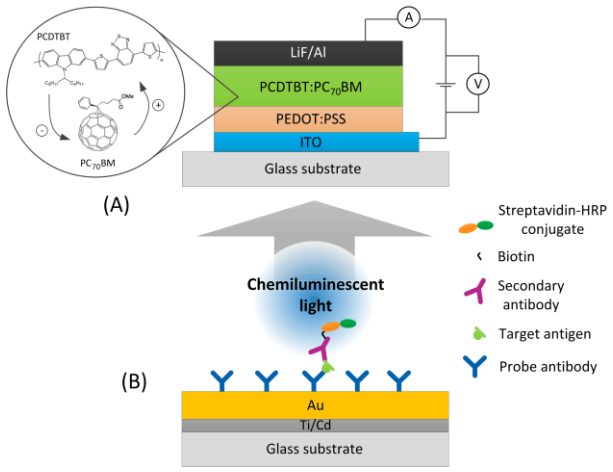

Figure 1. Biosensing scheme. The measurement module consists of two parts: (A) the ITO/PEDOT:PSS/PCDTBT:$PC_{70}BM$/LiF/Al photodiode; (b) chemiluminescent immunoassay chip with biomolecules immobilized on the Au coated glass substrate. Light (~425nm) is emitted from reaction of the luminescent substrate with the horseradish peroxidase (HRP) label.

The organic photodiodes with a photoactive area of 0.16 cm^2 were prepared on 1 mm ITO-coated glass substrates. After the substrates were pre-treated with UV ozone, the poly(3,4-ethylenedioxythiophene):polystyrene sulfonate (PEDOT:PSS) layer was spin coated on top of the substrates. The spin speed was varied between 1200 and 4500 rpm, resulting in film thicknesses from 80 nm down to 25 nm. Then the active layer of PCDTBT and $PC_{70}BM$ was deposited onto PEDOT:PSS layer by spin-coating from a 1:4 blend of two components in chloroform. The resultant film structures with active layer thicknesses between 70 and 180 nm were transferred into a N_2-glove box and dried at 60°C for 1 h. An Ambios XP-100 profilometer was used to measure the film thicknesses. The cathode electrodes were formed by thermal evaporation of LiF/Al (~100 nm) under 3×10^{-4} Pa. Subsequently, the photodiodes were encapsulated with a customized single-sided pressure-sensitive barrier foil [8, 9].

For preparation of the chemiluminescent immunoassays, reservoirs (~400 µl capacity) made of poly(dimethylsiloxane) (PDMS) were attached to the reaction chip and OPD slide, with the OPD placed above the reaction chip. Thus, the chemiluminescent light irradiates the bottom side of the photodiode (see Fig. 1). The immunoassays were performed on the surface of the Au-coated glass chip. All assay reagents are prepared from deionized water. First, the chip surface was coated by anti-rhTSH monoclonal antibody (probe antibody). Then the blocking buffer solution (diluted in phosphate buffered saline (PBS) with 0.05% Tween-20) blocked the residual reaction sites. The antibody-coated chip were incubated with rhTSH (varying concentration in PBS), and, subsequently washed with PBS. Thereafter, the biotinylated secondary antibody was added to the chip. After incubation and subsequent PBS washing, the immune complex interacted with streptavidin-conjugated horseradish peroxidase (HRP). The working solution, prepared by mixing equal parts of SuperSignal ELISA Femto Luminol/Enhancer and SuperSignal ELISA Femto Stable Peroxide Solution (Thermo Scientific), were transferred to the chip and interacted with the HRP conjugate. Finally, the photocurrent due to the chemiluminescence emission was measured with a computer-controlled Keithley 236 Source Measure Unit. All experiments were performed in the dark.

III. Results & Discussion

Firstly, the chemiluminescent signal was analyzed utilizing different thicknesses for the active layer. The thickness of PCDTBT:$PC_{70}BM$ was ranged between 70 and 180 nm, whilst the thickness of PEDOT:PSS layer was fixed at 50 nm. The chemiluminescent immunoassays were realized using a rsTSH concentration of 10 ng/ml, and generated photocurrent was measured under short circuit conditions. Besides, the external quantum efficiency (EQE) of PCDTBT:$PC_{70}BM$ devices was characterized for comparison. In this case, the photocurrent measurements were performed under irradiation from a xenon light source and a monochromator (Beijing Zolix Instruments Co., Ltd). System calibration was performed against a Si photodiode. Results for wavelengths ranging from 400 to 500 nm are shown in Fig. 2. Enhanced photocurrent was obtained for a PCDTBT:$PC_{70}BM$ thickness of 120 nm, which corresponded to increased EQE. The results for photocurrent due to chemiluminescent light emission (~425 nm) correlated well with the EQE spectra. The decreasing of EQE for thicknesses ranging from 120 to 180 nm is mainly due to the limited charge carrier mobilities in the active layer.

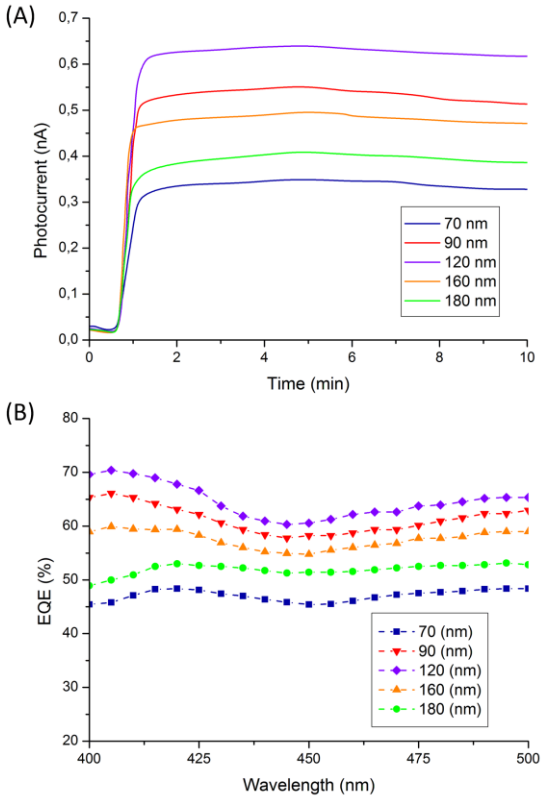

Figure 2. (A) Transient chemiluminescent signal detected by the polycarbazole photodiode at different PCDTBT:$PC_{70}BM$ thicknesses; (B) External quantum efficiency (EQE) for the PCDTBT:$PC_{70}BM$ devices.

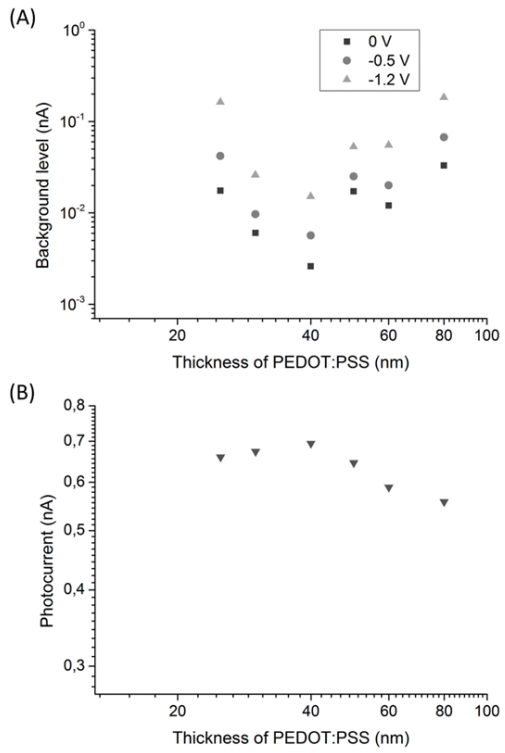

Figure 3. (A) Background current for the PCDTBT:$PC_{70}BM$ photodetector at different PEDOT:PSS film thicknesses; (B) Photocurrent at min 5 of the assay as a function of PEDOT:PSS thickness.

The effect of different PEDOT:PSS thickness on the performance of the chemiluminescent biosensor, in particular background signal and photosensitivity, has been studied. Devices with PEDOT:PSS thickness varying between 25 and 80 nm were compared, keeping PCDTBT:$PC_{70}BM$ thickness constant (120 nm). The background photocurrent was measured before adding the working solution to the immunoassay. Five minutes after the addition of the solution, it was analyzed the photocurrent in the plateau region of the chemiluminescent response signal. For assay development, 10 ng/ml of rsTSH was utilized in all measurements.

Fig. 3a shows the background level at different applied reverse bias as a function of PEDOT:PSS thickness. The minimum background photocurrent (~2.6 pA) was obtained for a film thickness of 40 nm, which corresponded to around one-fold improvement over a thickness of 50 nm. This mainly resulted from the decreasing of the dark current for the photodiode device. Recorded photocurrent at the plateau is shown in Fig. 3b. The amount of current increases clearly with decreasing PEDOT:PSS thickness, down to a thickness of 40 nm. Further decrease of thickness below 40 nm causes the photocurrent to drop slightly. Increase of photocurrent for film thickness between 80 and 40 nm may have been a direct consequence of increasing EQE, which in turn may have been due to the enhancement of chemiluminescent light absorption by the photodiode device. The PCDTBT:$PC_{70}BM$ device was thus optimized with a PEDOT:PSS thickness of 40 nm and an active layer thickness of 120 nm as a tentative to maximize the analytical sensitivity and reduce the LOD for the assay.

Prior to assessing the detection sensitivity of the chemiluminescent biosensor, the concentration of streptavidin-HRP was also optimized. The immunoassay was exposed to streptavidin-HRP concentrations between 5 and 25 ng/ml. The concentration of probe antibody was set as 0.1 µg/ml. From these experiments, a streptavidin-HRP concentration of 15 ng/ml was found to be optimal in terms of maximizing the signal-to-noise ratio. The results presented in Fig. 4 showed consistent for five rhTSH concentrations. Here, the signal-to-noise ratio was defined as the photocurrent taken from the plateau (5 min of the chemiluminescent assay) divided by the background level. The optimization of the streptavidin-HRP concentration may have led to decreasing the shot noise of the system, which may be related to statistical fluctuations in the photon flux density caused by the discrete nature of the photons. This kind of noise is relevant when it is aimed to detect low photocurrents [10].

Changes in the Current-Voltage curve due to the detection of different rhTSH concentrations were recorded for the polycarbazole photodiode. Fig. 5a shows the photocurrent dependence on the rhTSH concentration with applied bias voltage. Here, the photocurrent data were obtained from the plateau region of the chemiluminescent response signal. The response signal was characterized as shown in Fig. 2a. Testing analyte concentrations ranged from 2 to 120 ng/ml, and the assay was enhanced using 15 ng/ml of streptavidin-HRP. As evidenced in Fig. 5a, the photocurrent showed a remarkable increase with an increase in rhTSH concentration. For a 10 ng/ml concentration, the photocurrent was about fourty-fold higher compared to the reference value obtained from a non-rhTSH concentration.

Further, the short-circuit current was plotted against the concentration of rhTSH and the data are presented in Fig. 5b. A linear relationship between the analyte concentration and the photocurrent was encountered for seven concentrations between 0.1 and 5 ng/ml. To demonstrate the linearity, a correlation coefficient of 0.995 was obtained. Moreover, from the slope of the calibration curve, the detection sensitivity was calculated to be around 3.7 $nA \times nM^{-1}$ for the detection of rhTSH.

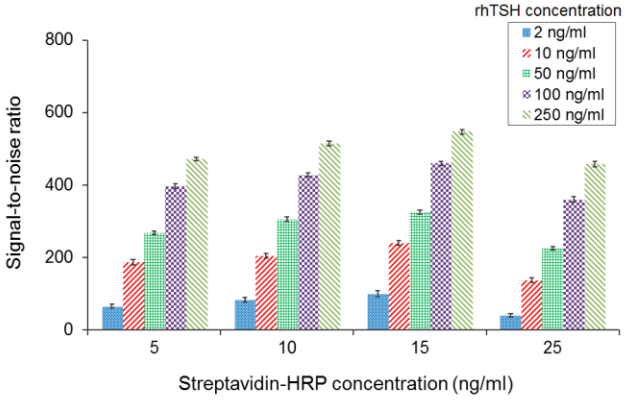

Figure 4. Optimization of the streptavidin-HRP concentration by determining the signal-to-noise ratio for a range of rhTSH concentrations. Error bars represent the standard deviation for triplicate measurements.

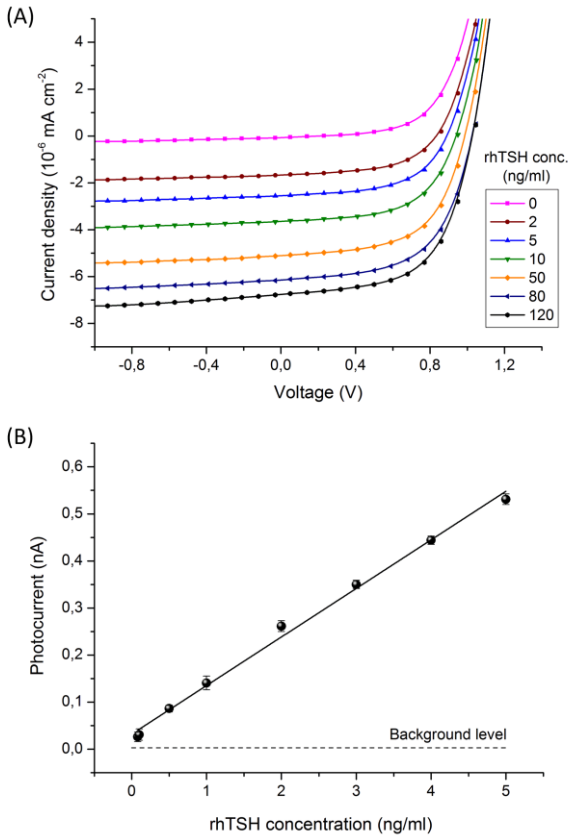

Figure 5. (A) Changes in the Current-Voltage curve due to the rhTSH concentrations, which were observed using the polycarbazole photodiode with 120-nm-thick PCDTBT:$PC_{70}BM$ and 40-nm-thick PEDOT:PSS; (B) Calibration curve for the detection of rhTSH by plotting the short-circuit current against the concentration of rhTSH. In this curve, the error bars correspond to the standard deviation for triplicate experiments.

The LOD for the chemiluminescent biosensor was 80 pg/ml or 2.25 pM. Further optimization of the PCDTBT:$PC_{70}BM$ photodetector might be conducted aiming to enhance the LOD, which would be promising to, for instance, detect very low concentrations of thyroid-stimulating hormone. The lower limit of the TSH reference range is typically 7 pg/ml.

IV. Conclusions and Outlooks

A chemiluminescent immunoassay using a polycarbazole-based photodiode as the optical detector was developed. The OPD device was comprised of a blend heterojunction of PCDTBT and $PC_{70}BM$, arranged with a structure of ITO/PEDOT:PSS/PCDTBT:$PC_{70}BM$/LiF/Al. Firstly, the OPD was optimized with a PCDTBT:$PC_{70}BM$ and PEDOT:PSS film thickness of 120 and 40 nm, respectively. Further, for assay optimization, a streptavidin-HRP concentration of 15 ng/ml was set before performing quantitative detection tests. Using rhTSH, a marker for diagnosis of thyroid cancer, as the model target, high detection sensitivity and very low LOD (tens of pg/ml) was verified. Thus, the PCDTBT:$PC_{70}BM$ photodetector would be promising for low level detection of important proteins or biomarkers.

Ongoing work currently involves the integration of the OPD with microfluidic chip structures, as a tentative to realize compact photodetector devices for in-the-field measurements. Furthermore, it is envisaged the realization of a high-throughput device comprising an array platform of OPDs. The envisaged device may offer a low-cost solution for multiplexed bioanalytical assays with potentially wide-ranging applications for POC diagnostics.

Acknowledgment

This work is mainly supported by Norsk regional kvalifiseringsstøtte fra Oslofjorfondet (Et cellebasert digitalt mikrofluidisk system, prosjekt nr: 220635). The Research Council of Norway is acknowledged for the support to the Norwegian Micro- and Nano-Fabrication Facility, NorFab (197411/V30), Norwegian long term support from NorFab project (Fabrication of nano-refinery for biomedical applications). The authors thank Nanjing University of Science & Technology, Institute of Hydrobiology in Chinese Academy of Sciences, and Xiamen University for assisting the experimental activities and covering part of their costs. The authors also appreciate the support and discussions from both co-supervisors Ph.D., Professor Nils Høivik and Ph.D., Professor Ulrik Hanke.

References

[1] B. Kuswandi, Nuriman, J. Huskens, and W. Verboom, "Optical sensing systems for microfluidic devices: a review," *Anal. Chim. Acta*, vol. 601, pp. 141-155, Oct. 2007.

[2] X. Zhao, T. Dong, Z. Yang, N. Pires, and N. Hoivik, "Compatible immuno-NASBA LOC device for quantitative detection of waterborne pathogens: design and validation," *Lab Chip*, vol. 12, pp. 602-612, Jan. 2012.

[3] A. Pais, A. Banerjee, D. Klotzkin, and I. Papautsky, "High-sensitivity, disposable lab-on-a-chip with thin-film organic electronics for fluorescence detection," *Lab Chip*, vol. 8, pp. 794-800, Mar. 2008.

[4] X. Wang, O. Hofmann, R. Das, E. M. Barrett, A. J. deMello, J. C. deMello, and D. D. C. Bradley, "Integrated thin-film polymer/fullerene photodetectors for on-chip microfluidic chemiluminescence detection," *Lab Chip*, vol. 7, pp. 58-63, May 2007.

[5] A. J. Heeger, "Semiconducting polymers: the third generation," *Chem. Soc. Rev.*, vol. 39, pp. 2354-2371, Jan. 2010.

[6] N. M. M. Pires, T. Dong, Z. Yang, N. Høivik, and X. Zhao, "A mediator embedded micro-immunosensing unit for electrochemical detection on viruses within physiological saline media," *J. Micromech. Microeng.*, vol. 21, 115031, Nov. 2011.

[7] T. Dong, Q. Su, Z. Yang, Y. Zhang, E. B. Egeland, D .D. Gu, P. Calabrese, M. J. Kapiris, F. Karlsen, N. T. Minh, K. Wang, and H. Jakobsen, "A smart fully integrated micromachined separator with soft magnetic micro-pillar arrays for cell isolation," *J. Micromech. Microeng.*, vol. 20, 115021, Nov. 2010.

[8] T. Dong, Z. Yang, Q. Bi, and Y. Zhang, "Freon R141b flow boiling in silicon microchannel heat sinks: experimental investigation," *Heat Mass Transfer*, vol. 44, pp. 315-324, Jan. 2008.

[9] T. Dong and Z. Yang, "Measurement and modeling of R141b condensation heat transfer in silicon rectangular microchannels," *J. Micromech. Microeng.*, vol. 18, 085012, Aug. 2008.

[10] J. Huang and J. deMello, "An introduction to organic photodetectors," in *Organic Electronics in Sensors and Biotechnology*, R. Shinar and J. Shinar, Ed. New York: McGraw-Hill, 2009, pp. 193-263.